Comput. Aided Geom. Des. 111 (2024) 102342

Contents lists available at ScienceDirect

Computer Aided Geometric Design

journal homepage: www.elsevier.com/locate/cagd

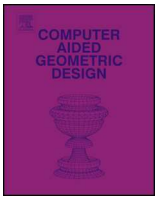

Hermite subdivision schemes for manifold-valued Hermite data

Hofit Ben-Zion Vardi, Nira Dyn, Nir Sharon *

School of Mathematical Sciences, Tel Aviv University, Tel Aviv, Israel

ARTICLE INFO

Keywords:
Manifold-Hermite approximation
De Casteljau algorithm
Manifold-Hermite data,
Manifold-Hermite Lane-Riesenfeld subdivision schemes

ABSTRACT

This paper introduces a family of subdivision schemes that generate curves over manifolds from manifold-Hermite data. This data consists of points and tangent directions sampled from a curve over a manifold. Using a manifold-Hermite average based on the De Casteljau algorithm as our main building block, we show how to adapt a geometric approach for curve approximation over manifold-Hermite data. The paper presents the various definitions and provides several analysis methods for characterizing properties of both the average and the resulting subdivision schemes based on it. Demonstrative figures accompany the paper's presentation and analysis.

1. Introduction

The problem of manifold-Hermite approximation of curves is approximating a curve that lies on a known manifold from a discrete data set of Hermite samples of the curve. We focus on first-order Hermite data consisting of samples taken from the curve, such that at each sample site, we are given both a point on the curve and the tangent direction at this point. The goal is to obtain a new manifold curve, which depends at each point on local samples and approximates the sampled curve. This paper describes a method for constructing such a curve using subdivision schemes based on the De Casteljau algorithm adapted to the manifold.

Manifold-Hermite approximation of manifold curves is a natural generalization of the problem of geometric Hermite approximation, where the data is given on a Euclidean domain. This problem extends the classical Hermite interpolation for functions, where the data consists of function value and its first derivative value at each sampling point. The geometric Hermite problem appears in many applications, among them curve design in Computer Aided Geometric Design (CAGD) (Xu and Shi, 2001), scientific simulations (Vargas et al., 2019), and Computer numerical control (CNC) (Beudaert et al., 2011), to name a few. Recent years brought up the manifold-Hermite settings both for curves (Moosmüller, 2016, 2017; Zimmermann, 2020) and multivariate manifold-valued functions (Zimmermann and Bergmann, 2023) and their relation to model reduction application (Zimmermann, 2021).

Our solution for the problem of manifold-Hermite approximation uses a generalized De Casteljau algorithm to define an intrinsic Riemannian average within the Hermite settings. Indeed, this is not the first attempt to utilize generalized De Casteljau algorithms for Riemannian manifold-valued data. An early work (Park and Ravani, 1995) shows the usage of Bézier curves via the De Casteljau for kinematics applications, and in Crouch et al. (1999), they apply the exponential map to define the De Casteljau process for Lie groups and spheres. In Rodrigues et al. (2005), the De Casteljau algorithm is utilized for generating smooth interpolating curves over Riemannian manifolds. Additional insights on the Riemannian De Casteljau are provided in Nava-Yazdani and Polthier (2013). A recent work (Zhang and Noakes, 2019) further adjusts the De Casteljau algorithm to obtain a variational interpolation called Riemannian cubics. While some of the above naturally addressed Hermite boundary conditions, the question of using the De Casteljau algorithm for tackling interpolation and approximation within the settings of the manifold-Hermite problem mainly remained open.

* Corresponding author.
E-mail addresses: hobenzion@gmail.com (H. Ben-Zion Vardi), niradyn@tauex.tau.ac.il (N. Dyn), nir.sharon@math.tau.ac.il (N. Sharon).

https://doi.org/10.1016/j.cagd.2024.102342

Available online 13 May 2024

The papers Moosmüller (2016, 2017) are the first to study Hermite subdivision schemes on manifolds specifically for solving the manifold-Hermite problem. In these papers, Moosmuller adapts linear Hermite subdivision schemes to manifold-valued Hermite data by several different methods. In contrast to this approach, we adapt a specific family of (non-linear) geometric subdivision schemes to manifolds, generating curves from Hermite data in $\mathbb{R}^n$ for any $n \in \mathbb{N}$. Our construction of curves in the geometric Hermite setting in $\mathbb{R}^n$, presented in Ben-Zion Vardi Hofit et al. (2023), begins with designing a geometric average. This fundamental building block, if chosen appropriately, allows us to apply the machinery of refinement via subdivision schemes. We adapt the linear Lane-Riesenfeld schemes generating splines to the Hermite-valued data by replacing the linear averages in these schemes with the geometric average. The limit of such a subdivision scheme generates a continuous curve whenever the scheme converges. We repeat this approach in the manifold-Hermite setting of the present paper.

In this paper, we first define what a manifold-Hermite average is. Then, we suggest such an average based on the De Casteljau algorithm for cubic Bézier curves adapted to manifolds with geodesics replacing line segments. We show several properties of this average and demonstrate it in two examples. Next, we incorporate our manifold-Hermite average as the average in the family of linear Lane-Riesenfeld schemes to produce curves over the manifold from the manifold-Hermite samples. We term these schemes generalized Lane-Riesenfeld schemes adapted to the manifold-Hermite setting. A careful analysis of our schemes reveals some of its properties, and in particular, we prove convergence via a tight connection to their Euclidean analogs in Ben-Zion Vardi Hofit et al. (2023), by the technique called *proximity*. Several numerical examples of our schemes over different manifolds accompany this part of the paper. We also introduce a more abstract framework for convergence analysis and approximation order of generalized Lane-Riesenfeld schemes to the manifold Hermite setting.

The paper is organized as follows. Section 2 introduces background materials needed for our construction: the De Casteljau algorithm, a short introduction to linear subdivision schemes, and the geometric Hermite problem in a Euclidean domain. Then, in Section 3, we formulate the manifold-Hermite problem we solve, define what manifold-Hermite averaging is, and present our manifold-Hermite average including its analysis and demonstration. Finally, Section 4 presents the application of our manifold-Hermite average in a Lane-Riesenfeld subdivision scheme. This section also consists of the convergence analysis of the scheme, a few theoretical considerations for manifold and manifold-Hermite schemes, and some numerical examples.

2. Background

We provide three subsections of background material essential to our study.

2.1. De Casteljau algorithm

The classic Bernstein operator that approximates $f : [0,1] \to \mathbb{R}$ from its equidistant samples is

$$B_N(f;x) = \sum_{i=0}^{N} b_{N,i}(x) f\left(\frac{i}{N}\right), \quad x \in [0,1],$$

where the basis functions are the polynomials

$$b_{N,i}(x) = \binom{N}{i} x^i (1-x)^{N-i}. \tag{2.1}$$

A standard numerical evaluation of $B_N(f;x)$ is done via the celebrated *De Casteljau* algorithm. This algorithm calculates the B_N operator's value in N rounds. We next describe it in detail.

As a first round of the De Casteljau algorithm, we define

$$\beta_i^0 = f\left(\frac{i}{N}\right), \quad i = 0, \dots, N.$$

Then, the following steps are arithmetic averages of the form

$$\beta_i^{j+1} = (1-x)\beta_i^j + x\beta_{i+1}^j, \quad i = 0, \dots, N-j, \quad j = 0, \dots, N-1.$$

The output is $\beta_0^N = B_N(f;x)$, where the correctness of the algorithm is based on the recursive relation:

$$b_{k,i}(x) = (1-x)b_{k-1,i}(x) + x b_{k-1,i-1}(x), \quad x \in [0,1].$$

Here, $b_{k,i}(x)$ is the Bernstein basis polynomial (2.1). We also present the De Casteljau algorithm as a pseudocode in Algorithm 1.

One crucial aspect of the above algorithm is the fact that $\beta_i^{j+1} = (1-x)\beta_i^j + x\beta_{i+1}^j$ is merely the x-weighted arithmetic average of β_i^j and β_{i+1}^j. Thus, we can generalize the De Casteljau algorithm by replacing the linear arithmetic means of numbers with other weighted means of other objects (e.g., point-tangent pairs) and thus obtain generalized Bernstein approximations.

An important special case to this paper is the evaluation of cubic Bézier curves, which are curves in $\mathbb{R}^n$ corresponding to N = 3 with $\{\beta_j^0\}_{j=0}^3$ replaced by $\{p_j^0\}_{j=0}^3$, where $\{p_j^0\}_{j=0}^3$ are points in $\mathbb{R}^n$.

Algorithm 1 The De Casteljau algorithm.

Require: $N+1$ samples $f_i = f\left(\frac{i}{N}\right)$, $i = 0, \ldots, N$, evaluation point $x \in [0,1]$,
Ensure: The value of $B_N(f;x)$.
1: **for** i = 0,..., N **do**
2: $\beta_i^0 = f\left(\frac{i}{N}\right)$
3: **end for**
4: **for** j = 0,..., N-1 **do**
5: **for** i = 0,..., N-j **do**
6: $\beta_i^{j+1} = (1-x)\beta_i^j + x\beta_{i+1}^j$
7: **end for**
8: **end for**
9: **return** β_0^N

2.2. A short introduction to linear subdivision schemes and approximation via refinement

In this paper, we deal with curves on manifolds, so we briefly review univariate subdivision schemes. Linear, univariate subdivision schemes operate on sequences of numbers and generate the limit graphs of univariate functions. These schemes generate curves in $\mathbb{R}^n$ for any n from a sequence of points (vectors) in $\mathbb{R}^n$ by operating on each component separately. A refinement rule of a univariate linear subdivision scheme S has the form

$$(S\mathbf{f})_i = \sum_{j\in\mathbb{Z}} \mathbf{a}_{i-2j}\mathbf{f}_j.$$

Here $\mathbf{f}$ and $S(\mathbf{f})$ are two sequences of real numbers defined on $\mathbb{Z}$, and $\mathbf{a}$ is a finite sequence of real numbers termed the mask of the scheme. The repeated application of the refinement rule of the scheme S to the sequence $\mathbf{f^0}$ leads to the sequences,

$$\mathbf{f}^{k+1} = S(\mathbf{f}^k), \quad k = 0, 1, \ldots.$$

A subdivision scheme S is called **convergent** if the sequence of piecewise linear interpolants to the data $\{(i2^{-k}, \mathbf{f}_i^k)\}_{i\in\mathbb{Z}}$, denoted by $\{F^k(t)\}_{k\in\mathbb{N}_0}$, converges uniformly to a limit function which is called the limit of the subdivision scheme S and denoted by $S^\infty\mathbf{f}^0$.

A subdivision S is called **interpolatory** if $(S\mathbf{f})_{2i} = \mathbf{f}_i$ for all $i \in \mathbb{Z}$. If such a scheme is convergent, then its limit curves interpolate the initial data.

An important family of univariate subdivision schemes are generating splines of degree m, $m \in \mathbb{N}$ with the masks

$$\mathbf{a}_i = 2^{-m}\binom{m+1}{i} t^i(1-t)^{m-i}, \quad i = 0, \ldots, m+1, \quad m \in \mathbb{N}.$$

There is a rather simple algorithm, the Lane-Riesenfeld algorithm of order $m, (LR_m)$, which uses only the arithmetic average of numbers with weight $\frac{1}{2}$. Therefore, this algorithm can be adapted to manifold-Hermite data by replacing the arithmetic mean with a manifold-Hermite average. Algorithm 2 describes the refinement step of the LR_m algorithm acting on points.

Assume a curve in $\mathbb{R}^n, C(t)$, is defined for $t \in [a,b]$. If the component of $\mathbf{f^0}$ is the samples of $C(t)$ at $t_i = a + ih$, $i = 0, \ldots, N$ with $h = \frac{b-a}{N}$, for some $N \in \mathbb{N}$, then the limit curve obtained by repeated applications of the refinement step of Algorithm 2 approximates $C(t)$ with an error of order $O(h)$.

Algorithm 2 The refinement step of the Lane-Riesenfeld of order m.

Require: The data points to be refined $\{p_i\}_{i\in\mathbb{Z}}$. The order m.
Ensure: The refined points.
1: **for** $i \in \mathbb{Z}$ **do** {elementary refinement}
2: $q_{2i}^0 \leftarrow p_i$
3: $q_{2i+1}^0 \leftarrow p_i$
4: **end for**
5: **for** $j = 1$ **to** m **do** {repeated averaging}
6: **for** $i \in \mathbb{Z}$ **do**
7: $q_i^j \leftarrow \frac{1}{2}\left(q_i^{j-1} + q_{i+1}^{j-1}\right)$
8: **end for**
9: **end for**
10: **return** $\{q_i^m\}_{i\in\mathbb{Z}}$

2.3. The geometric Hermite problem in $\mathbb{R}^n$

In this subsection, we briefly sketch our paper (Ben-Zion Vardi Hofit et al., 2023), which is the starting point of this paper. In the geometric Hermite problem in $\mathbb{R}^n$, $n \in \mathbb{N}$, we are given geometric Hermite data sampled from a G^1 curve $\gamma : I \to \mathbb{R}^n$, where I is a closed interval in $\mathbb{R}$. The G^1 continuity here means both the curve and its tangents are continuous. Then, we wish to construct an approximating curve $\widetilde{\gamma} \approx \gamma$ based on the available data.

The samples are in the form of geometric Hermite data over $\mathbb{R}^n$, namely a sequence

$$\left((p_j, v_j)\right)_{j\in\mathbb{Z}} \subseteq \mathbb{R}^n \times S^{n-1}, \tag{2.2}$$

where S^{n-1} is the $n-1$ sphere in $\mathbb{R}^n$, such that each sample consists of a point on the curve and a tangent direction to the curve at the point. In the geometric Hermite problem, we only take into account unit directions. This is because the magnitude of the tangent is not a geometric quantity, as it directly depends on the curve's parameterization. Therefore, different parameterizations can produce varying results. To mitigate these effects, we assume that the curve is sampled with respect to arc-length parameterization, and each tangent is measured to provide direction only.

Admissible Hermite data consists of admissible pairs of consecutive samples $(p_i, v_i), (p_{i+1}, v_{i+1})$, satisfying

$$p_i \neq p_{i+1}, \text{ and } v_i, v_{i+1}, u_i \text{ are not pair-wise linearly dependent, or } v_i = v_{i+1} = u_i, \tag{2.3}$$

with $u_i = (p_{i+1} - p_i)/\left\|(p_{i+1} - p_i\right\|$.

The admissibility condition guarantees that each consecutive pair of samples defines a regular Bézier curve, which is the main tool in defining an average between pairs of consecutive samples in Ben-Zion Vardi Hofit et al. (2023). This average, termed the Bézier average, is denoted by $B_\omega\left(Q_i, Q_{i+1}\right)$, with $Q_i = (p_i, v_i)$. It is obtained from the Bézier curve $b_i(t)$ based on the four control points

$$p_i,\ p_i + \alpha_E v_i,\ p_{i+1} - \alpha_E v_{i+1},\ p_{i+1}, \tag{2.4}$$

with $\alpha_E = \alpha_E(Q_i, Q_{i+1})$, the multiplier derived in Dokken et al. (1990), and used in Lipovetsky and Dyn (2016). By the admissibility condition, $b_i(\omega)$ is differentiable. Therefore, the tangent vector to $b_i(\omega)$ exists for all $\omega \in [0,1]$. In addition, when $b_i'(\omega) \neq 0$ we define $B_\omega(Q_i, Q_{i+1}) = \left(b_i(\omega), \frac{b_i'(\omega)}{\left\|b_i'(\omega)\right\|}\right)$.

It is shown in Ben-Zion Vardi Hofit et al. (2023) that the LR_1 algorithm with the Bézier average $B_{\frac{1}{2}}(\cdot,\cdot)$ replacing the arithmetic mean of points in step 7 of Algorithm 2, and with Hermite data as initial data for the algorithm, is a convergent subdivision scheme with G^1 limit curves interpolating the initial Hermite data. We denote the schemes in Ben-Zion Vardi Hofit et al. (2023) by $\mathcal{H}LR_m$, $m \in \mathbb{N}$.

Remark 2.1. About the Bézier average and its application to the Lane-Riesenfeld subdivision scheme $\mathcal{H}LR_m$:

1. The Bézier average with $\omega = \frac{1}{2}$ exists for all Hermite data satisfying (2.3), and is calculated by the De Casteljau algorithm with $N = 3, x = \frac{1}{2}$.
2. It is interesting to note that the limit tangent directions are the tangent directions of the limit curve in contrast to the algorithm in Lipovetsky and Dyn (2016).
3. It is concluded from numerical tests that if the initial Hermite data consists of the samples of a G^1 curve $\gamma : [0,1] \to \mathbb{R}^n$, the limit curve of the modified LR_1 approximates the sampled curve. In addition, the approximation order approaches $\mathcal{O}(h^4)$, similar to classical cubic Hermite interpolation. For more details, see Ben-Zion Vardi Hofit et al. (2023, Figure 7).

3. Hermite problem and Hermite averaging in the manifold setting

3.1. On manifolds and manifold averaging

Let $\mathcal{M}$ denote a (geodesically) complete Riemannian manifold of dimension $\dim \mathcal{M}$, and let $T_{\mathcal{M}}(p)$ denote the tangent space of $\mathcal{M}$ at a point $p \in \mathcal{M}$ and so the tangent bundle is the union of all tangent spaces, $T_{\mathcal{M}} = \cup_{p\in\mathcal{M}} T_{\mathcal{M}}(p)$. The completeness means that the exponential map at a point $p \in \mathcal{M}$ is defined for any vector in $T_{\mathcal{M}}(p)$.

A curve over $\mathcal{M}$ is a function $\Gamma : I \to \mathcal{M}$ where $I \subset \mathbb{R}$ is a real, closed segment. We say that Γ is G^1 if it satisfies this regularity as a Euclidean curve in $\mathbb{R}^n$ when viewing $\mathcal{M}$ an embedded submanifold of $\mathbb{R}^n$ and the derivatives are taken in extrinsic coordinates.

The Riemannian metric of $\mathcal{M}$ is the collection of all local inner product $\langle\cdot,\cdot\rangle_p$ for every point $p \in \mathcal{M}$. Each inner product induces a norm over the tangent space $T_{\mathcal{M}}(p)$, $\|\cdot\|_p$. In this paper, we omit the subscript p when it is clear from the context. Here, we denote by $d_{\mathcal{M}}(p,q)$, $p, q \in \mathcal{M}$ the Riemannian distance over $\mathcal{M}$, defined as the length of the minimal length curve, on the manifold, connecting p and q, and measured using the Riemannian metric. We denote the exponential map of a vector v in the tangent space $T_{\mathcal{M}}(b)$, $b \in \mathcal{M}$, and its inverse logarithm map by

$$q = b \oplus v = \mathrm{Exp}_b(v), \quad \text{and} \quad v = q \ominus b = \mathrm{Log}_b(q), \quad b, q \in \mathcal{M}. \tag{3.1}$$

Namely, $b \oplus v$ maps a vector $v \in T_{\mathcal{M}}(b)$ to the point on the manifold which lies at a distance $\|v\|$ along the geodesic line from b which is tangent to v. On the other hand, $q \ominus b$ seeks the vector $v \in T_{\mathcal{M}}(b)$ such that $b \oplus v = q$. If q is inside the injectivity radius (where the exponential map is one-to-one), then $b \oplus (q \ominus b) = q$ and the distance, $\rho_{\mathcal{M}}(b,q)$, is merely $\|q \ominus b\|$, with the Euclidean norm in $T_{\mathcal{M}}(b)$. Note that the completeness of $\mathcal{M}$ here means that $\mathrm{Exp}_b(v)$ is well-defined for any $v \in T_{\mathcal{M}}(b)$.

A manifold intrinsic weighted average (mean) between two points is a function $\mathrm{AV} : I \times \mathcal{M} \times \mathcal{M} \to \mathcal{M}$, where $I \supseteq [0,1]$ is the domain of the weights. We assume that $I = [0,1]$ for simplicity. We require any intrinsic average to satisfy the following:

1. Identity on the diagonal: $\mathrm{AV}(\omega; p, p) = p$, $\omega \in [0, 1]$.
2. Symmetry: $\mathrm{AV}(\omega; p, q) = \mathrm{AV}(1-\omega; q, p)$.
3. End points interpolation: $\mathrm{AV}(0; p, q) = p$ and $\mathrm{AV}(1; p, q) = q$.

The above properties may be interpreted as an extension of the properties of the linear arithmetic average of numbers, $(1-\omega)r + \omega s$, where $s, r \in \mathbb{R}$.

Since $\mathcal{M}$ is complete, any two points are connected by at least one geodesic line. In the rest of the paper, we assume that any two points to be averaged in our algorithms are such that there is a unique geodesic curve connecting them. Under this assumption, the geodesic mean is a natural choice of a manifold intrinsic weighted average. We denote this geodesic average by $G_{\mathcal{M}}(\omega; p, q)$. Note that when ω varies between 0 and 1, the geodesic average defines the geodesic curve (shortest path) connecting p and q over $\mathcal{M}$. One may verify that the geodesic average is indeed a manifold intrinsic weighted average.

3.2. Hermite problem for manifold-valued curves

Manifold-Hermite data over $\mathcal{M}$ refers to a sequence

$$\left((p_j, v_j) \in \mathcal{M} \times S^{n-1}(p_j)\right)_{j\in\mathbb{Z}}, \tag{3.2}$$

where $S^{n-1}(p_j)$ is the $(n-1)$-sphere centered at p_j in the Euclidean space $T_{\mathcal{M}}(p_j)$, equipped with the angular metric, and $n = \dim \mathcal{M}$. Note that the assumption $J = \mathbb{Z}$ is posed for simplicity since it helps us avoid the technical treatment of special boundary rules. In practice, one may use a finite set of indices of the form $J = \{0, 1, \ldots, N\}$ with $N \in \mathbb{N}$ when viewing such a sequence as samples of an $\mathcal{M}$-valued G^1 curve. Note that similar to the geometric Hermite problem of Section 2.3, we consider only tangent directions.

The problem we consider is the following:

Definition 3.1 *(The manifold-Hermite problem for curves).* Consider a G^1 curve $\gamma : \mathbb{R} \to \mathcal{M}$. Given its manifold-Hermite samples $\left((p_j, v_j)\right)_{j\in\mathbb{Z}}$ of the form,

$$p_j = \gamma(t_j), \quad v_j = \frac{\dot{\gamma}(t_j)}{\left\|\dot{\gamma}(t_j)\right\|}, \quad j \in \mathbb{Z}. \tag{3.3}$$

Here, $t_j < t_{j+1}$, $j \in \mathbb{Z}$, and v_j is the normalized tangent to γ at the parametric point t_j. Our aim is to find a curve $\widetilde{\gamma} : \mathbb{R} \to \mathcal{M}$ which approximates γ.

When addressing the above manifold-Hermite problem, we assume we sample a curve. Here, we suggest some regularization conditions on the samples to obtain *admissible Hermite data*.

Definition 3.2. A set of manifold-Hermite data is called *admissible* if, there exists a positive constant, $\Theta < 2\pi$, such that for any two consecutive data elements, $(p_i, v_i), (p_{i+1}, v_{i+1})$, the corresponding angles defined in (3.7), satisfy

$$\theta_0 + \theta_1 \le \Theta < 2\pi. \tag{3.4}$$

In addition, we assume that $p_i \neq p_{i+1}$, for any $i \in \mathbb{Z}$, and that any two such points lie within the injectivity radius where the exponential map from one to the other is one-to-one.

Note that while Definition 3.2 requires that any two points will be within the injectivity radius, in practice, we can relax this requirement. Instead, we can define a local injectivity radius that will ensure the existence of geodesics within the data's vicinity. For simplicity, we have omitted the formulation and usage of this technical requirement.

Henceforth, if not otherwise stated, we assume any manifold-Hermite data is admissible.

Remark 3.3. Two comments regarding Definition 3.2:

1. When sampling manifold-Hermite data from a geodesic line, we obtain $\theta_0 + \theta_1 = 0$ for any consecutive data pair; see the proof of Proposition 3.6. Therefore, the requirement in (3.4) basically indicates that the samples are close enough. Indeed, in such a scenario, we analyze the convergence of the subdivision scheme LR_1, adapted to manifold Hermite data by replacing the linear average with the manifold-Hermite De Casteljau average. (See Section 4.3)
2. In $\mathbb{R}^n$, the conditions in (2.3) ensure that $\theta_0 + \theta_1 < 2\pi$. Here, we further ask that this sum is bounded away from 2π.

For the following, we update our notation for the usage of parallel transport along geodesics. This transport moves a vector along a geodesic curve over a Riemannian manifold such that its derivative is orthogonal to the manifold; see, e.g., Petersen (2006, Chapter 6). Specifically, for $v \in T_{\mathcal{M}}(p)$, we denote by $PT_{\mathcal{M}}(p; v, q)$ the vector in $T_{\mathcal{M}}(q)$ which is the result of the parallel transport of v along the geodesic connecting p and q.

The next notion of **manifold-Hermite average for manifold-Hermite data** is central to how we solve the manifold-Hermite problem.

Definition 3.4. We term H_w a manifold-Hermite average over $\mathcal{M}$ if it maps pairs of manifold-Hermite data to a single element of manifold-Hermite data and if it satisfies the following conditions for any $w \in [0,1]$ and $(p_j, v_j) \in \mathcal{M} \times S^{n-1}(p_j)$, $j = 0, 1$:

1. *Identity on the v-directional diagonal.* Let $(p, v) \in \mathcal{M} \times S^{n-1}(p)$ and denote by $p_t = p \oplus tv$ a geodesic shift of p over $\mathcal{M}$ with $t \geq 0$. Also, denote the parallel transport of v to p_t by $v_t = PT_{\mathcal{M}}\left(p; v, p_t\right)$. Then,

$$H_w\left((p, v), (p_t, v_t)\right) \xrightarrow{t \longrightarrow 0^+} (p, v).$$

2. *Symmetry with respect to orientation.*

$$\text{If} \quad H_w\left((p_0, v_0), (p_1, v_1)\right) = (p, v) \quad \text{then} \quad H_{1-\omega}\left((p_1, -v_1), (p_0, -v_0)\right) = (p, -v).$$

3. *Endpoints interpolation.*

$$H_0\left((p_0, v_0), (p_1, v_1)\right) = (p_0, v_0) \quad \text{and} \quad H_1\left((p_0, v_0), (p_1, v_1)\right) = (p_1, v_1).$$

In the next subsection, we introduce such an average and show that it is a manifold-Hermite average.

3.3. The manifold-Hermite De Casteljau average

Let $Q_0 = (p_0, v_0)$ and $Q_1 = (p_1, v_1)$ be two manifold-Hermite data elements. We term our manifold-Hermite average **manifold-Hermite De Casteljau average** and denote it by $\mathcal{DH}_w\left((p_0, v_0), (p_1, v_1)\right)$. This average is constructed following the next steps:

1. Define two auxiliary points:

$$\widetilde{p_j} = p_j \oplus (-1)^j \alpha v_j, \quad j = 0, 1, \tag{3.5}$$

with

$$\alpha = \alpha(Q_0, Q_1) = \frac{d_{\mathcal{M}}\left(p_0, p_1\right)}{3\cos^2\left(\frac{\theta_0 + \theta_1}{4}\right)}, \tag{3.6}$$

where

$$\theta_0 = \arccos\left(\frac{\langle v_0, p_1 \ominus p_0\rangle_{p_0}}{\|p_1 \ominus p_0\|}\right) \quad \text{and} \quad \theta_1 = \arccos\left(\frac{\langle v_1, -p_0 \ominus p_1\rangle_{p_1}}{\|p_0 \ominus p_1\|}\right). \tag{3.7}$$

2. Apply the De Casteljau algorithm (Algorithm 1) with $N = 3$ and $x = w$ to the four points $p_0, \widetilde{p_0}, \widetilde{p_1}, p_1$, using as average the manifold geodesic mean $G_{\mathcal{M}}(w; \cdot, \cdot)$ to obtain the point of the average q.
3. The vector of the average u is the normalized tangent at the point q to the geodesic line connecting the two points p_0^2, p_1^2, generated in the second round of the De Casteljau algorithm in the previous step. Note that this tangent can be defined by connecting u to either endpoint p_0^2 or p_1^2 up to a sign. Therefore, for any $w \neq 1$ we defined it with p_1^2, and for $w = 1$ we do it with p_0^2 and negative sign. These two definitions are equivalent for any $w \in (0, 1)$.
4. Finally, $\mathcal{DH}_w\left((p_0, v_0), (p_1, v_1)\right) = (q, u)$.

Two notes regarding the above algorithm. First, for the Hermite case in $\mathbb{R}^n$, α is the same parameter from Ben-Zion Vardi Hofit et al. (2023), computed fully in the Euclidean space. In this paper, we denote it by α_E (see Section 2.3) and use α when it is computed over $\mathcal{M}$. Second, the auxiliary points (3.5) carry into the averaging process the information of the tangent vectors. This process is summarized in Algorithm 3.

Proposition 3.5. *The average $\mathcal{DH}_w(\cdot, \cdot)$ is a manifold-Hermite average.*

Proof. We must show that $\mathcal{DH}_w$ satisfies the three conditions in Definition 3.4. For the first, in the notation there, we note that $p_t = p \oplus tv$ lies on the geodesic which starts at p and is tangent to v at p. Therefore, for small t values, $p_t \ominus p = tv$ and also $\left(\frac{\langle v, tv\rangle_p}{\|tv\|}\right) = 1$. These two observations imply that θ_ℓ of (3.7) vanishes as $\arccos 1 = 0$. Similar arguments lead to $\theta_r = 0$, where θ_r is also defined in (3.7). By (3.6) $\alpha(Q, Q_t) = \frac{\|tv\|}{3} = \frac{t}{3}$, where $Q = (p, v)$ and $Q_t = (p_t, v_t)$.

Keeping t small, we have in $\mathcal{DH}(Q, Q_t)$

$$p_0^0 = p, \; p_1^0 = p \oplus \frac{1}{3}tv, \; p_2^0 = p_t \oplus (-\frac{1}{3})tv = p \oplus \frac{2}{3}tv, \; p_3^0 = \; p_t = p \oplus tv,$$

Algorithm 3 The manifold-Hermite De Casteljau average.

Require: Two manifold-Hermite data: $(p_0, v_0), (p_1, v_1)$ and a weight w
Ensure: The average (q, u).
1: Calculate α of (3.6)
2: Define $p_0^0 = p_0, \quad p_1^0 = p_0 \oplus \alpha v_0, \quad p_2^0 = p_1 \oplus (-\alpha v_1), \quad p_3^0 = p_1$
3: Compute $p_j^1 \leftarrow G_{\mathcal{M}}\left(w; p_j^0, p_{j+1}^0\right), \quad j = 0, 1, 2$
4: Compute $p_j^2 \leftarrow G_{\mathcal{M}}\left(w; p_j^1, p_{j+1}^1\right), \quad j = 0, 1$
5: $q \leftarrow G_{\mathcal{M}}\left(w; p_0^2, p_1^2\right)$
6: **if** $w \neq 1$ **then**
7: $\quad u \leftarrow \frac{p_1^2 \ominus q}{\left\|p_1^2 \ominus q\right\|}$
8: **else if** $w = 1$ **then**
9: $\quad u \leftarrow \frac{p_0^2 \ominus q}{-\left\|p_0^2 \ominus q\right\|}$
10: **end if**
11: **return** (q, u)

and following Algorithm 3, we get

$$p_0^1 = p \oplus \frac{w}{3} tv, \; p_1^1 = p \oplus \frac{1+w}{3} tv, \; p_2^1 = p \oplus \frac{2+w}{3} tv, \; p_0^2 = p \oplus \frac{2w}{3} tv, \; p_1^2 = p \oplus \frac{1+2w}{3} tv.$$

Finally, $q = p \oplus wtv$ and for both $w \neq 1$ and $w = 1$, we have $u = PT_{\mathcal{M}}(p; v, p \oplus wtv)$ since we stay on the geodesic connecting p and $p \oplus wtv$. Thus, as t tends to zero $q = p$ and $u = v$, and so the first condition holds.

For the symmetry condition, observe first that α has the same value in the $\mathcal{DH}_{1-w}$ case as in the original $\mathcal{DH}_w$ case. Then, in the $1 - w$ case, the first four points become $p_1, p_1 \oplus (-\alpha v_1), p_0 \oplus \alpha v_0$, and p_0. Namely, a mirror (opposite) order of the initial four points in the $\mathcal{DH}_w$ case. Now, the symmetry follows directly from the same symmetry satisfied by the geodesic mean, namely, $G_{\mathcal{M}}(w; a, b) = G_{\mathcal{M}}(1 - w; b, a)$.

For the proof of the third condition on endpoints interpolation, we consider first the case $w = 0$. Following Algorithm 3, we get $p_j^1 = p_j^0$, for $j = 0, 1, 2$ and $p_i^2 = p_i^1 = p_i^0$, for $i = 0, 1$ Thus $q = p_0^2 = p_0^1 = p_0$. Since $p_1^2 = p_1^1 = p_1^0 = p_0 \oplus \alpha v_0$, we get by step 7 of Algorithm 3 that $u = v_0$.

The case $w = 1$ is similar with $p_j^1 = p_{j+1}^0$ for $j = 0, 1, 2$, and $p_i^2 = p_{i+1}^1$ for $i = 0, 1$. Thus $q = p_1^2 = p_2^1 = p_3^0 = p_1$. Since $p_0^2 = p_1^1 = p_2^0 = p_1 \ominus \alpha v_1$, we get by step 9 of Algorithm 3 that $u = v_1$. □

3.4. Properties of the manifold-Hermite De Casteljau average

The proof of Proposition 3.5, and in particular the proof of the first condition about identity on the v-directional diagonal, reveals yet another property of the manifold-Hermite De Casteljau average: it reproduces geodesics, namely, when the two points and tangents are sampled from a geodesic line then their manifold-Hermite De Casteljau average is a sample of that geodesic. This is stated more precisely in the next Proposition.

Proposition 3.6. *Let p_0 and p_1 be connected by a unique geodesic in $\mathcal{M}$ and let v_0, v_1 be tangents of this geodesic, at the points p_0 and p_1 respectively, that is*

$$v_0 = \frac{p_1 \ominus p_0}{\left\|p_1 \ominus p_0\right\|} \quad \text{and} \quad v_1 = -\frac{p_0 \ominus p_1}{\left\|p_0 \ominus p_1\right\|}. \tag{3.8}$$

Then, for all $w \in [0, 1]$ the manifold component of $\mathcal{DH}_w\left((p_0, v_0), (p_1, v_1)\right)$ is the point on the geodesic given by $G_{\mathcal{M}}\left(w; p_0, p_1\right)$, and the vector component is tangent to this geodesic at the point $G_{\mathcal{M}}\left(w; p_0, p_1\right)$.

Proof. By (3.8) we have that $\theta_0 = \theta_1 = 0$, see (3.7). Therefore, (3.6) implies that $\alpha = \frac{\left\|p_1 \ominus p_0\right\|}{3}$. Thus, the calculation process of the De Casteljau-Hermite average starts with

$$p_0^0 = p_0, \quad p_1^0 = G_{\mathcal{M}}\left(1/3; p_0, p_1\right), \quad p_2^0 = G_{\mathcal{M}}\left(2/3; p_0, p_1\right), \quad p_3^0 = p_1.$$

Then, Algorithm 3 continues with

$$p_0^1 = G_{\mathcal{M}}\left(w/3; p_0, p_1\right), \quad p_1^1 = G_{\mathcal{M}}\left((1+w)/3; p_0, p_1\right), \quad p_2^1 = G_{\mathcal{M}}\left((2+w)/3; p_0, p_1\right),$$

and

$$p_0^2 = G_{\mathcal{M}}\left((2w)/3; p_0, p_1\right) \quad \text{and} \quad p_1^2 = G_{\mathcal{M}}\left((1+2w)/3; p_0, p_1\right).$$

Note that all the points calculated by Algorithm 3 are on the geodesic. Finally, $q = G_{\mathcal{M}}\left((w; p_0^2, p_1^2\right) = G_{\mathcal{M}}\left((w; p_0, p_1\right)$, namely q lies on the geodesic connecting p_0 with p_1. By the definition of the tangent, it is clear that it is tangential to the geodesic at q. □

Next, we show the connection between the manifold-Hermite De Casteljau average and its Euclidean counterpart. Here, we lay the first step towards a proximity analysis done later in Section 4.3. In what follows, where possible, we omit the constants for simplicity and use the big-O notation, $f = \mathcal{O}(g)$ if $f \leq C \cdot g$, as g and f tend to zero. We mention the factors involved in C in cases where it is required or nontrivial.

Lemma 3.7. *Let $\mathcal{M} \subset \mathbb{R}^n$, and consider a pair of manifold-Hermite data $Q_0 = (p_0, v_0), Q_1 = (p_1, v_1)$. Denote by $d := d_{\mathcal{M}}(p_0, p_1)$ and assume that d and $\theta_0 + \theta_1$ of (3.7) are sufficiently small. Then,*

$$\left\| \mathcal{DH}_w(Q_0, Q_1) - B_w(Q_0, Q_1) \right\| = O(d^2), \quad w \in (0,1). \tag{3.9}$$

Here the norm is the Euclidean norm in $\mathbb{R}^n$, and $B_w(Q_0, Q_1)$ for $w \in (0,1)$, is the unique cubic Bézier curve that interpolates the Hermite data in $\mathbb{R}^n$ given by $(p_0, \alpha_E v_0)$ and $(p_1, \alpha_E v_1)$, with $\alpha_E = \alpha(Q_0, Q_1)$ of (3.6) taken with respect to $\mathbb{R}^n$.

Proof. Based on the observation (see e.g., Wallner and Dyn (2005, Appendix C)), that there exist constants C_1 and C_2 such that for small enough t, when $v \in T_{\mathcal{M}}(p_0)$ is considered also as a vector in $\mathbb{R}^n$,

$$\|(p_0 \oplus tv) - (p_0 + tv)\| \leq C_1 t^2 \quad \text{and} \quad \left\| G_{\mathcal{M}}(w; p_0, p_1) - ((1-w)p_0 + wp_1) \right\| \leq C_2 d^2. \tag{3.10}$$

Thus, for any $\tilde{p}_0, \tilde{p}_1 \in \mathcal{M}$ such that $d_{\mathcal{M}}(p_j, \tilde{p}_j) = O(d^2)$, $j = 0, 1$, it holds that $\left\| p_j - \tilde{p}_j \right\| = O(d^2)$ and

$$\begin{aligned} &\left\| G_{\mathcal{M}}(w; p_0, p_1) - ((1-w)\tilde{p}_0 + w\tilde{p}_1) \right\| \\ &\leq \left\| G_{\mathcal{M}}(w; p_0, p_1) - ((1-w)p_0 + wp_1) \right\| + \|((1-w)p_0 + wp_1) - ((1-w)\tilde{p}_0 + w\tilde{p}_1)\| \\ &\leq C_2 d^2 + \max_{j=0,1} \{ \left\| p_j - \tilde{p}_j \right\| \} = O(d^2) \end{aligned} \tag{3.11}$$

Next, we follow the notation and computational process in Algorithm 3 for $\mathcal{DH}_w((p_0, v_0), (p_1, v_1))$ and in Algorithm 1 with $N = 3$ for $B(w)$. First, since $\theta_0 + \theta_1$ is close to zero, we have that $\alpha(p_0^0, p_3^0) \approx \alpha_E(\beta_0^0, \beta_3^0)$. In particular, it means that using (3.10), the calculation of $B_w(Q_0, Q_1)$ starts with

$$\beta_0^0 = p_0^0, \quad \beta_3^0 = p_3^0, \quad \beta_1^0 = p_0^0 + \alpha_E(\beta_0^0, \beta_3^0) v_0, \quad \beta_2^0 = p_3^0 - \alpha_E(\beta_0^0, \beta_3^0) v_1.$$

Namely, since $\alpha_E(\beta_0^0, \beta_3^0) = O(\left\| \beta_0^0 - \beta_3^0 \right\|)$ for small $\theta_0 + \theta_1$, we have that $\left\| \beta_1^0 - p_1^0 \right\|, \left\| \beta_2^0 - p_2^0 \right\| = O(d^2)$ by (3.10). Therefore, following (3.11), we get that $\left\| p_j^1 - \beta_j^1 \right\| = O(d^2)$, $j = 0, 1, 2$ and as a consequence $\left\| p_j^2 - \beta_j^2 \right\| = O(d^2)$, $j = 0, 1$, and the lemma follows. □

Lemma 3.7 shows how close the point values of our average $\mathcal{DH}_w$ are to those of the cubic Bézier curve in the ambient Euclidean space, corresponding to the same w. We further investigate this relation after introducing the application of our average to the generation of manifold curves in Section 4.

We continue with characterizing the distances generated by our average. Specifically, we measure distances by the Riemannian metric of our manifold $\mathcal{M}$ and explore the resulting distances between the average point q of the manifold-Hermite De Casteljau average and the averaged points p_0, p_1.

The first step is followed by the admissibility condition (3.4) that provides us with the next lemma.

Lemma 3.8. *If the manifold-Hermite data satisfies (3.4), then, for any two consecutive points p_j, p_{j+1} their multiplier α in the De Casteljau-Hermite average $\alpha(Q_j, Q_{j+1})$ satisfies*

$$\alpha(Q_j, Q_{j+1}) \leq C(\Theta) d_{\mathcal{M}}(p_j, p_{j+1}), \quad C(\Theta) = \frac{1}{3\cos^2\left(\frac{\Theta}{4}\right)}. \tag{3.12}$$

Proof. By (3.4), $\frac{\theta_0+\theta_1}{4} \leq \frac{\Theta}{4} \leq \frac{\pi}{2}$, and cosine is monotonically decreasing in $[0, \frac{\pi}{2})$ so $\cos\left(\frac{\theta_0+\theta_1}{4}\right) \geq \cos\left(\frac{\Theta}{4}\right)$. Then, the result follows from (3.6). □

Now, we follow the De Casteljau algorithm to obtain a bound on the required distances.

Lemma 3.9. *Let $Q_j = (p_j, v_j)$, $j = 0, 1$, and let $\alpha(Q_0, Q_1) = \frac{d_{\mathcal{M}}(p_0,p_1)}{3\cos^2(\frac{\theta_0+\theta_1}{4})}$ as defined in (3.6). In the notation of Algorithm 3,*

$$\max\{d_{\mathcal{M}}(p_0, q), d_{\mathcal{M}}(p_1, q)\} \leq \alpha(Q_0, Q_1) + \frac{1}{2} d_{\mathcal{M}}(p_1^0, p_2^0).$$

The proof is given in Appendix A.

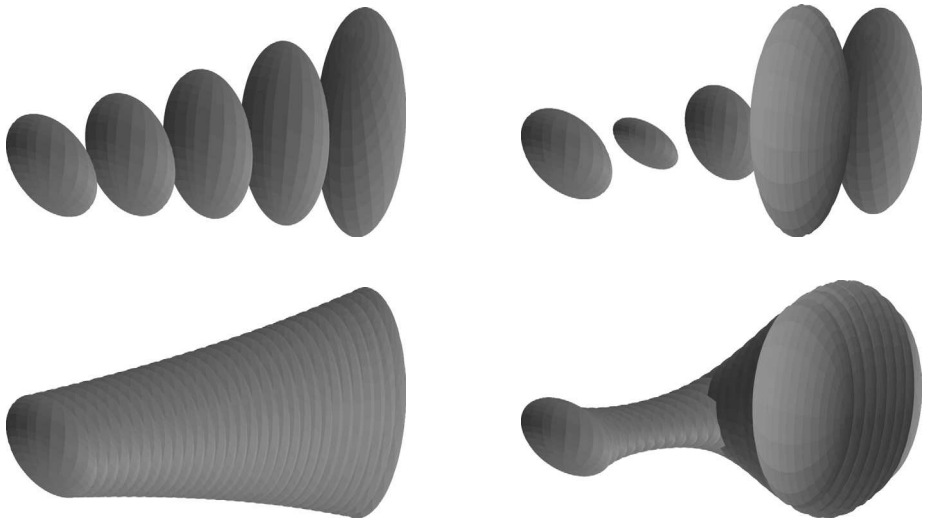

Fig. 1. Two examples of manifold-Hermite De Casteljau average over the 3×3 positive definite matrices cone. In each example, we present the matrices as ellipsoids and depict the resulting average in two resolutions, as the text explains. In Example 1 (left), we sample a Riemannian geodesic connecting two matrices. In Example 2 (right), we average a pair consisting of the same points as in the previous example, but this time, they are associated with arbitrary tangent directions.

Lemma 3.9 implies that the distance $d_{\mathcal{M}}\left(p_1^0, p_2^0\right)$ has a key role. A naive bound is

$$\begin{aligned} d_{\mathcal{M}}\left(p_1^0, p_2^0\right) &\le d_{\mathcal{M}}\left(p_0 \oplus (\alpha v_0), p_0\right) + d_{\mathcal{M}}\left(p_0, p_1\right) + d_{\mathcal{M}}\left(p_1, p_1 \oplus (-\alpha v_1)\right) \\ &= 2\alpha(Q_0, Q_1) + d_{\mathcal{M}}\left(p_0, p_1\right). \end{aligned} \tag{3.13}$$

The above (3.13) together with (3.12) entails that

$$d_{\mathcal{M}}\left(p_j, q\right) \le (2C(\Theta) + 1) d_{\mathcal{M}}\left(p_0, p_1\right), \quad j = 0, 1.$$

This bound separates the distance between the average and the averaged values into two factors. One factor depends on the angles, and the other is the distance between the averaged points.

3.5. Visualizing the manifold-Hermite De Casteljau average

To conclude this section, we provide in Fig. 1 a visual illustration of the manifold-Hermite De Casteljau average, operating over the manifold (cone) of positive definite matrices. In this illustration, we present two examples of the average, where only the matrices (without the tangent directions) are depicted as ellipsoids whose axes are given by the eigenvectors and of length determined by the corresponding eigenvalues. Each example consists of two different resolutions of the weight w, one with $w = 0, \frac{1}{4}, \frac{1}{2}, \frac{3}{4}, 1$ and the other with $w = \frac{k}{30}, k = 0, 1, \ldots, 30$.

In the first example, we present a geodesic between two chosen matrices p_0 and p_1 and average the two pairs $\left(p_0, \frac{p_1 \ominus p_0}{\|p_1 \ominus p_0\|}\right)$ and $\left(p_1, \frac{p_0 \ominus p_1}{-\|p_0 \ominus p_1\|}\right)$. Note that geodesics are unique in the manifold of positive definite matrices, and any of them can be extended beyond their two endpoints to remain geodesic. These settings are similar to Proposition 3.5 that proves the reproducibility of geodesics.

In the second example, we use the same end-point matrices p_0 and p_1. However, instead of taking the tangents of the geodesic, we picked two arbitrary directions, describing sampling a curve that is different from the geodesic. The result is very different averaged matrices (and tangents, although they are not shown in this figure).

Next, we describe the construction of a manifold curve from manifold-Hermite data via refinement.

4. Generating manifold curves from manifold-Hermite samples by refinements

This section describes how we use the manifold-Hermite De Casteljau average to address the manifold-Hermite problem for curves of Definition 3.1. Specifically, we use subdivision schemes adapted to Hermite manifold values as our main tool for approximating the manifold curves, employing a refinement process in each step of the subdivision scheme based on our manifold-Hermite De Casteljau average. This section includes numerical examples. The complete Python source code is available online in https://github.com/HofitVardi/Manifold-Hermite-approximation.

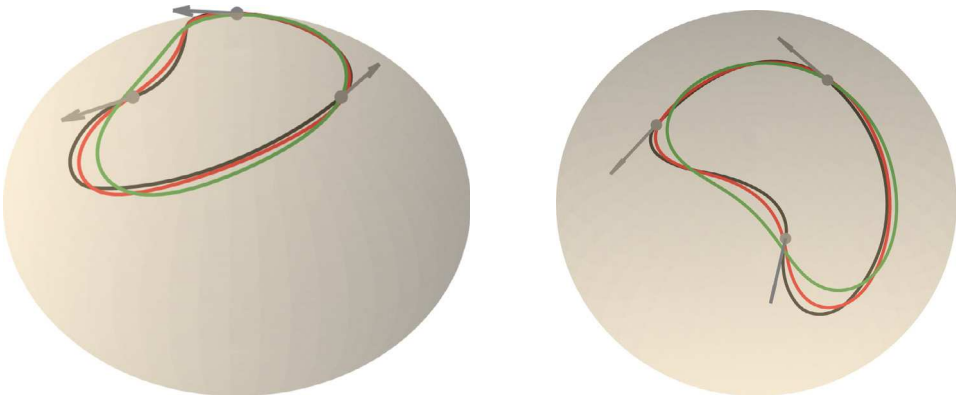

Fig. 2. Limit curves of $\mathcal{M}_H LR_m$ schemes of 3 different orders over the sphere from two different viewing angles. Gray: initial data, black: $\mathcal{M}_H LR_1$, red: $\mathcal{M}_H LR_3$, green: $\mathcal{M}_H LR_{10}$. (For interpretation of the colors in the figure(s), the reader is referred to the web version of this article.)

4.1. Manifold-Hermite Lane-Riesenfeld subdivision schemes

While subdivision schemes can be adapted to manifold values differently (see, e.g., Moosmüller (2016, 2017)), we focus on defining a Lane-Riesenfeld type refinement, which generalizes B-splines for manifold-Hermite problems. The basic building block is a manifold-Hermite average, which in our case is the manifold-Hermite De Casteljau average $\mathcal{DH}_{\omega}(\cdot,\cdot)$ with $\omega = \frac{1}{2}$.

Each refinement step is done similarly to Algorithm 2 but now adjusted to manifold values. Recall that the order m indicates how many rounds of averaging are applied. In particular, as m grows, each value of refinement depends on more data points. This version of the LR_m algorithm based on the average $\mathcal{DH}_{\frac{1}{2}}(\cdot,\cdot)$ is given in Algorithm 4, where we present each Hermite manifold data (p,v) by the letter Q.

Algorithm 4 The refinement step of the manifold-Hermite Lane-Riesenfeld of order m.

Require: The manifold-Hermite data to be refined $\{(p_i,v_i)\}_{i\in\mathbb{Z}}$. The order m.
Ensure: The refined data.
for $i\in\mathbb{Z}$ **do**
  $Q^0_{2i} \leftarrow (p_i,v_i)$
  $Q^0_{2i+1} \leftarrow (p_i,v_i)$
end for
for $j=1$ **to** m **do**
  for $i\in\mathbb{Z}$ **do**
    $Q^j_i \leftarrow \mathcal{DH}_{\frac{1}{2}}\left(Q^{j-1}_i, Q^{j-1}_{i+1}\right)$
  end for
end for
return $\{Q^m_i\}_{i\in\mathbb{Z}}$

Repeated refinements with Algorithm 4 are a subdivision scheme adjusted to manifoldHermite data. We denote it by $\mathcal{M}_H LR$.

In Fig. 2, we demonstrate the limit curves generated by three different $\mathcal{M}_H LR$ schemes, corresponding to orders $m = 1, 3, 10$. The manifold here is the sphere in $\mathbb{R}^3$.

Next, we analyze some of the basic properties of the $\mathcal{M}_H LR_m$ scheme and its resulting limits. As a first result, we present the property of geodesic reproduction, directly inherited by the $\mathcal{M}_H LR_m$ schemes from the manifold-Hermite De Casteljau average as the latter reproduces geodesics by Proposition 3.6.

Corollary 4.1. *Suppose the manifold-Hermite data is sampled from a unique geodesic. Then, the $\mathcal{M}_H LR_m$ schemes, for any $m\in\mathbb{N}$, converge to the geodesic line.*

In the next subsection, we recall tools and results from Dyn and Sharon (2017b) on manifold Lane-Riesenfeld schemes, refining manifold-valued data and adding to it an approximation theorem on these schemes.

4.2. Analysis of manifold Lane-Riesenfeld schemes and an approximation result

We recall the notion of convergence for manifold-valued subdivision schemes. Namely, schemes that refine sequences of manifold points (without considering tangent directions). In this manifold setting, the refinement schemes generate sequences of points of manifold values, starting from the initial data $\mathbf{p}^0 = \{p^0_j\}_{j\in\mathbb{Z}}$ and generating by repeated refinements the sequences $\mathbf{p^k} = \{p^k_j\}_{j\in\mathbb{Z}}$, $k = 1, 2, \ldots$. For the analysis, we recall the notion

$$\Delta\mathbf{p} := \sup_{j\in\mathbb{Z}} d_{\mathcal{M}}\left(p_j, p_{j+1}\right), \tag{4.1}$$

and assume that the initial data has a finite supremum, namely that $\Delta\mathbf{p}^0 < \infty$.

Recall $F^k(t)$, the piecewise linear interpolant of $\mathbf{f}^k$ in linear subdivision schemes (see Section 2.2). On a manifold, we define $F^k(t)$ to be the piecewise geodesic curve interpolating the data $(i2^{-k}, p_i^k)$, $i \in \mathbb{Z}$, such that the points of any two consecutive data elements in $\mathbf{p}^\mathbf{k}$ are connected by a geodesic. Note that this curve lies on the manifold.

Then, in analogy to the linear schemes case, the scheme is called **convergent**, if the sequence of manifold-valued curves $\{F^k(t)\}_{k\in\mathbf{N}}$ is a Cauchy sequence, and the limit of this sequence is called **the limit curve generated by the scheme S from the initial data $\mathbf{P^0}$**. By Dyn and Sharon (2017b), to prove the convergence of a manifold scheme, it is sufficient to prove that the scheme satisfies the two conditions of contractivity and displacement-safe (D-S).

Formally, these two conditions for convergence are read as follows: a scheme S is called contractive if there exists a contractivity factor $\mu \in (0,1)$, depending on S, such that

$$\Delta\left(\{S(\mathbf{p})_j\}_{j\in\mathbb{Z}}\right) \le \mu\Delta\mathbf{p}. \tag{4.2}$$

The D-S condition means that there exists a constant C, depending on S, such that

$$d_{\mathcal{M}}\left(S(\mathbf{p})_{2j}, p_j\right) \le C\Delta\mathbf{p}, \quad j\in\mathbb{Z}. \tag{4.3}$$

By definition, any interpolatory scheme automatically satisfies the D-S condition (with $C = 0$).

In Dyn and Sharon (2017a), we study a wide family of manifold-valued subdivision schemes obtained from linear schemes. In particular, we adapt the family of linear LR schemes to manifold-valued data. We denote the resulting schemes by $\mathcal{MLR}_m$. With respect to the linear Algorithm 2, in these schemes the linear average with weight $\frac{1}{2}$ between points is replaced by the geodesic average $G_{\mathcal{M}}\left(\frac{1}{2};\cdot,\cdot\right)$.

The geodesics, as the shortest paths, together with the Riemannian metric $d_{\mathcal{M}}$, satisfy the **metric property**,

$$d_{\mathcal{M}}\left(G_{\mathcal{M}}\left(w;p_0,p_1\right),p_1\right) = (1-w)d_{\mathcal{M}}\left(p_0,p_1\right), \quad p_0,p_1\in\mathcal{M}, \quad w\in[0,1]. \tag{4.4}$$

This important property plays a significant role in analyzing $\mathcal{MLR}_m$. Specifically, it is shown that $\mu = \frac{1}{2}$ is the contractivity factor of any $\mathcal{MLR}_m$ scheme. In such cases, we can further prove a new result (not obtained in Dyn and Sharon (2017a)) that $\mathcal{MLR}_m$ approximates the sampled curve at least in the rate $O(h)$. For this, we recall a result from the manifold comparison theory. In Dekster (1980), curves on manifolds of bounded sectional curvatures were considered. In particular, for a manifold of curvature bounded by K, one uses a compared auxiliary manifold of a curvature value equal to K. There, the overall length of the original curve can be compared to the circumference of a ball in the compared manifold, which in turn can be computed explicitly. The curve's curvature is defined as the derivative of the tangents, as measured at the tangent space; see, for example, Castrillón López et al. (2010, Section 3). Note that there is a mild restriction on the curvature of the curve at each point so that it will fit into the comparison conditions. We denote this bound by $\kappa(K)$, as in the Dekster (1980, Theorems in §1) and refer the interested reader for more details in Dekster (1977, 1980). We summarize the result in the following theorem.

Theorem 4.2. *Assume $\mathcal{M}$ has sectional curvatures bounded from above by K. Let $\gamma:\mathbb{R}\to\mathcal{M}$ be a piecewise C^2 curve with the curvature at every point bounded by $\kappa(K)$. For given manifold-Hermite data $\mathbf{p}^0$ which are samples of γ, define $h = \Delta\mathbf{p}^0$. If a manifold-valued subdivision scheme S satisfies the D-S condition and has a contractivity factor $\mu = \frac{1}{2}$, then*

$$d_{\mathcal{M}}\left(S^\infty(\mathbf{p})(t),\gamma(t)\right) \le C\,h, \quad t\in\mathbb{R}.$$

Here $C = 1 + 2C_{DS} + C_\gamma$, where C_{DS} is the D-S constant of S and C_γ is a constant depending on K and the curvature of γ.

Proof. For short we use $S^\infty(t) = S^\infty(\mathbf{p})(t)$. Let $t\in[t_j,t_{j+1})$, with t_j, t_{j+1} parameter values corresponding to level zero. Then, we have

$$d_{\mathcal{M}}\left(S^\infty(t),\gamma(t)\right) \le d_{\mathcal{M}}\left(S^\infty(t),S^\infty(t_j)\right) + d_{\mathcal{M}}\left(S^\infty(t_j),\gamma(t_j)\right) + d_{\mathcal{M}}\left(\gamma(t_j),\gamma(t)\right).$$

We divide the remaining proof according to the three terms. Starting with the first, we observe that any parameter value at the kth level in the interval $[t_j,t_{j+1}]$, corresponding to points in this level, is of the form $\tau_i = t_j + 2^{-k}i$, $i = 0,\ldots,2^k-1$. Therefore,

$$d_{\mathcal{M}}\left(S^k(\tau_i),S^k(t_j)\right) \le i\cdot\Delta\mathbf{p}^k \le 2^k\mu^k\Delta\mathbf{p}^0 = \Delta\mathbf{p}^0, \quad i = 0,1,\ldots,2^k-1.$$

Taking the limit $k\to\infty$, we obtain $d_{\mathcal{M}}\left(S^\infty(t),S^\infty(t_j)\right)\le h$, for any $t\in[t_j,t_{j+1}]$. To bound the second term, first recall that $\gamma(t_j) = p_j^0$. Then, observe the kth level and apply the D-S and contractivity to get,

$$\begin{aligned} d_{\mathcal{M}}\left(S^k(t_j),\gamma(t_j)\right) &\le d_{\mathcal{M}}\left(p^k_{2^k j},p^{k-1}_{2^{k-1}j}\right) + \ldots + d_{\mathcal{M}}\left(p^1_{2j},p^0_j\right) \\ &= \sum_{\ell=0}^{k-1} d_{\mathcal{M}}\left(p^\ell_{2^\ell j},p^{\ell+1}_{2^{\ell+1}j}\right) \end{aligned}$$

$$\leq C_{DS}\left(\sum_{\ell=0}^{k-1}\Delta\mathbf{p}^{\ell}\right)\leq C_{DS}\Delta\mathbf{p}^{0}\left(\sum_{\ell=0}^{k-1}\mu^{\ell}\right)\leq\left(\frac{C_{DS}}{1-\mu}\right)\Delta\mathbf{p}^{0}.$$

However, the right-hand side is independent of k. Therefore, taking the limit $k\to\infty$ we obtain

$$d_{\mathcal{M}}\left(S^{\infty}(t_j),\gamma(t_j)\right)\leq(2C_{DS})h.$$

Finally, denote the length of the curve γ between two parametric values a,b by $L_{\gamma}(a,b)$. Since geodesics are the shortest paths and $t<t_{j+1}$, we have

$$d_{\mathcal{M}}\left(\gamma(t_j),\gamma(t)\right)\leq L_{\gamma}(t_j,t)\leq L_{\gamma}(t_j,t_{j+1}).$$

Now, we use the comparison theorem for curves on manifolds of bounded sectional curvature (Dekster, 1980) to conclude that there exists a constant C_{γ} such that the latter length is bounded by

$$L_{\gamma}(t_j,t_{j+1})\leq C_{\gamma}d_{\mathcal{M}}\left(\gamma(t_j),\gamma(t_{j+1})\right)\leq C_{\gamma}\Delta\mathbf{p}^{0}=C_{\gamma}h.\quad\square$$

We conclude this subsection with another notion, called *proximity*, related to convergence. In particular, in Wallner and Dyn (2005), it is proven that if S is a linear subdivision scheme and T is its manifold counterpart, and if the schemes satisfy the proximity condition,

$$\left\|S(\mathbf{p}_0)-T(\mathbf{p}_0)\right\|_{\infty}\leq C(\Delta\mathbf{p}_0)^2,\tag{4.5}$$

for any dense enough set $\mathbf{p}_0$ of data, then convergence of S is inherited by T, and under a minor technical condition on S, if S generates C^1 limits so does T.

4.3. The convergence of the interpolatory manifold-Hermite Lane-Riesenfeld via proximity

We recall the schemes in Ben-Zion Vardi Hofit et al. (2023), $\mathcal{H}LR_m$, which are the Euclidean analog of our $\mathcal{M}_H LR_m$ scheme; see Section 2.3. We further develop the results in Lemma 3.7 to harness the proximity between the averages for proximity between the schemes. This analysis eventually leads to point convergence of $\mathcal{M}_H LR_m$, inherited by the convergence of $\mathcal{H}LR_m$. Note that the convergence in Ben-Zion Vardi Hofit et al. (2023) is shown only for the case $m=1$. In the following result, we use the notation $\theta_j=\theta_j(Q_0,Q_1)$, $j=0,1$ when referring to (3.7). In addition, when applying the average directly over $\mathbb{R}^n$ to obtain values of Bézier curves, we use $\theta_j^E(Q_0,Q_1)$, $j=0,1$. These angles are the ones in use in $\mathcal{H}LR_m$.

Our next proximity result shows that not only the manifold values attend first-order proximity (as stated in Lemma 3.7) but also the angles. This is crucial for two main reasons. First, it means that we can apply this one-step refinement proximity iteratively since angle proximity appears as a condition for the point proximity. Second, it indicates that under proximity, the θ_0,θ_1 angles tend to zero. Note that the angle proximity is of one order lower than the point proximity. This is expected, as the angles arise from the tangents, which are the derivatives of the curve values that we compare.

Theorem 4.3. *Consider $\mathcal{M}\subset\mathbb{R}^n$ and denote by θ_j^E, $j=0,1$ the angles of (3.7) in $\mathbb{R}^n$. Let Q_0,Q_1 be a pair of manifold-Hermite data satisfying*

$$\theta_j(Q_0,Q_1),\ \theta_j^E(Q_0,Q_1)\ll 1,\quad j=0,1\quad\text{and}\quad d:=d_{\mathcal{M}}\left(p_0,p_1\right)\ll 1.\tag{4.6}$$

Denote the values of the averages by $Q_{\frac{1}{2}}=(q,u):=\mathcal{DH}_{\frac{1}{2}}\left(Q_0,Q_1\right)$ and $B_{\frac{1}{2}}=(b,v):=B_{\frac{1}{2}}(Q_0,Q_1)$. Then,

$$\|q-b\|=O(d^2),\tag{4.7}$$

where the norm is taken in $\mathbb{R}^n$, and

$$\left|\theta_j(Q_0,Q_{\frac{1}{2}})-\theta_j^E(Q_0,B_{\frac{1}{2}})\right|,\ \left|\theta_j(Q_{\frac{1}{2}},Q_1)-\theta_j^E(B_{\frac{1}{2}},Q_1)\right|=O(d),\quad j=0,1.\tag{4.8}$$

The proof is given in Appendix B.

Theorem 4.3 shows the connection between the geometric Hermite averaging in $\mathbb{R}^n$ using the Bézier curve and our manifold-Hermite average. In Ben-Zion Vardi Hofit et al. (2023), we show that the interpolatory $\mathcal{H}LR_1$, which is based on the Bézier curve averaging, is convergent with a contractivity factor. Therefore, utilizing proximity, we obtain the following conclusion:

Corollary 4.4. *The sequence of points generated by $\mathcal{M}_H LR_1$ converges to a continuous limit curve in $\mathcal{M}$ for dense enough initial data points.*

Proof. Following the same arguments from Wallner and Dyn (2005, Theorem 2), we obtain that the contractivity factor for the sequence of points generated by $\mathcal{H}LR_1$ leads to a contractivity factor for the points in $\mathcal{M}_H LR_1$, if the initial data is dense enough. Therefore, in view of Section 4.2, since $\mathcal{M}_H LR_1$ is interpolatory, convergence follows. $\square$

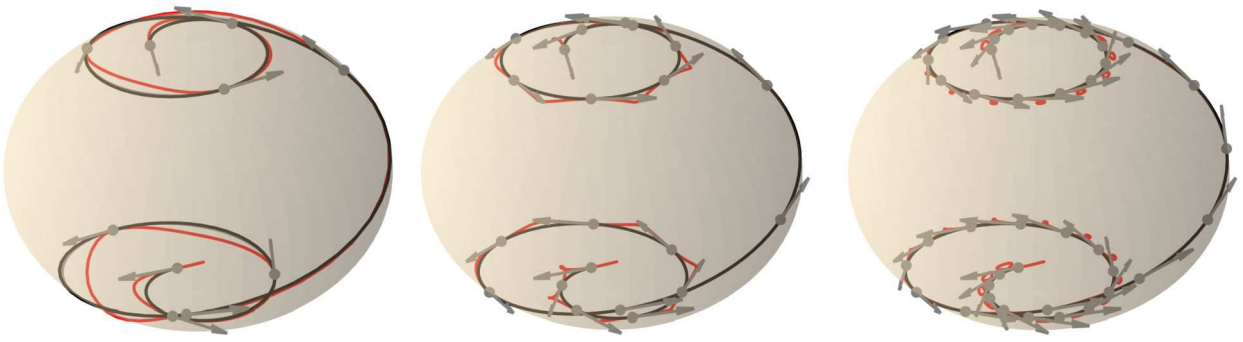

Fig. 3. Approximations of a spherical spiral by $\mathcal{M}_H LR_1$ (black) and by a manifold's analog of a linear Hermite subdivision scheme via parallel transport (Moosmüller, 2017) (red). The true curve and initial data are presented in gray. Each of the figures uses a different sampling rate.

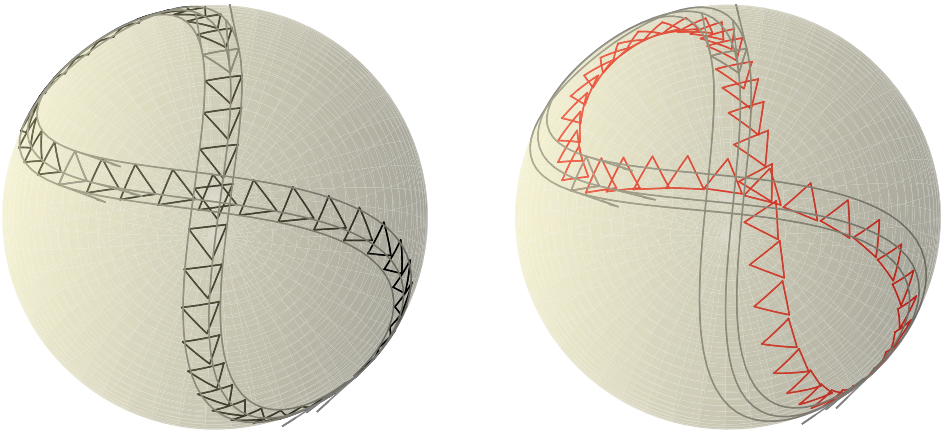

Fig. 4. Approximations of a curve over SO(3) by $\mathcal{M}_H LR_1$ (left) and by a manifold's analog of a linear Hermite subdivision scheme via parallel transport (Moosmüller, 2017) (right). The action of the sampled curve over a fixed spherical triangle is given as three eight-shaped grey curves, each indicates the continuous change of one triangle vertex by the action of the elements of SO(3) along the curve. The sampling location is identified where the grey tangents appear. The approximation curves are given only on a finite set of locations where the rotated triangle is displayed.

Although for the convergence of the points in Corollary 4.4 we use only (4.7) from Theorem 4.3, the angle proximity (4.8) is also required to guarantee the conditions (4.6) when we apply (4.7) iteratively.

In Ben-Zion Vardi Hofit et al. (2023), it is shown that the angles θ_0^E, θ_1^E between the tangents and the piecewise linear polygon that connects the points tend to zero as the level of refinement increases. The conclusion there is that the tangent directions in the limit are tangent to the limit of the points. Here, since θ_0^E, θ_1^E and θ_0, θ_1 are connected by (4.8), we deduce that θ_0, θ_1 also tend to zero.

Corollary 4.5. *Assume the initial manifold-Hermite data is dense enough. If the tangent directions generated by $\mathcal{M}_H LR_1$ are converging, then the limit tangents are tangent to the point limit curve, and this limit curve is G^1.*

We conclude this part with two interpolatory $\mathcal{M}_H LR_1$ examples. In the first example in Fig. 3, we consider samples of a spiral over the sphere in $\mathbb{R}^3$. Then, we compare our $\mathcal{M}_H LR_1$ and a manifold's analog of Hermite subdivision scheme via parallel transport (Moosmüller, 2017). The results show two smooth-looking curves, where the $\mathcal{M}_H LR_1$ limit gives a visually preferred approximation.

In the second example, in Fig. 4, we consider a curve over the Lie group of orientation-preserving 3-D rotations, SO(3). We visualize the curve by applying its action on a fixed spherical triangle. The sampled curve is depicted by three continuous curves, which indicate the triangle's vertices at each point along the curve. In the sampling location, the tangent samples also appear. As in the previous example, we compare our $\mathcal{M}_H LR_1$ scheme with the solution in Moosmüller (2017). Each approximation is presented only on a discrete set of points by showing the resulting rotated triangle at the depicted point. A good approximation is identified when the vertices of the triangles are located close to the three continuous curves. Again, our scheme provides a preferred approximation, which lies very close to the sampled curve.

4.4. General considerations about convergence in the setting of manifold-Hermite

Starting with a manifold-Hermite average H_w, and two manifold-Hermite points $Q_0 = (p_0, v_0)$ and $Q_1 = (p_1, v_1)$, we define the induced curve by H_w, connecting Q_0 and Q_1, as

$$C : [0,1] \to \left(\mathcal{M}, S^{m-1}\right), \quad C(w) = H_w(Q_0, Q_1), \quad 0 \le w \le 1. \tag{4.9}$$

Clearly, this curve depends on the endpoints, that is, $C(w) = C_{Q_0,Q_1}(w)$; however, for brevity, we use the extended notation only if needed.

Assuming further that $\dot{C}(w) = \frac{d}{dw}C(w) \in \left(T_{\mathcal{M}} \times T_{S^{m-1}}\right)$ exists almost everywhere. In addition, we define the norm of the derivative $\left\|\dot{C}(w)\right\|$ as the sum of the Euclidean norm in each tangent space. Finally, we define the curve length:

$$\mathcal{L}_H(Q_0, Q_1) = \int_0^1 \left\|\dot{C}_{Q_0,Q_1}(w)\right\| dw. \tag{4.10}$$

For the first convergence result, we assume two additional conditions; the first is a triangle inequality that could be applied for any three points over a curve with respect to $\mathcal{L}_H$. The second is a bound on the distance to the midpoint with respect to the endpoint distance according to $\mathcal{L}_H$. These assumptions are typical in cases of geodesic averages with respect to their associated metric. The theorem reads:

Theorem 4.6. *Assume the following:*

1. *For any manifold-Hermite data point, $Q \in \left(\mathcal{M}, S^{m-1}\right)$, $Q \neq Q_0, Q_1$*

$$\mathcal{L}_H(Q_0, Q_1) \le \mathcal{L}_H(Q_0, Q) + \mathcal{L}_H(Q, Q_1). \tag{4.11}$$

2. *There exists $\mu \in (0,1)$ such that*

$$\mathcal{L}_H(H_{\frac{1}{2}}(Q_0, Q_1), Q_j) \le \mu \mathcal{L}_H(Q_0, Q_1), \quad j = 0, 1. \tag{4.12}$$

Then, the interpolatory manifold-Hermite Lane-Riesenfeld, $\mathcal{M}_H LR_1$, that uses H_w as its average, converges from any admissible initial Hermite data.

Proof. We use the following lemma:

Lemma 4.7. *Under condition (4.11), the length $\mathcal{L}_H$ of (4.10) is a metric.*

(Proof of Lemma 4.7). We show the three conditions of a metric. First, by definition, the length is nonnegative. In addition, for any two distinct points, Q_0 and Q_1, by continuity of $C(w)$, the length is nonzero, and thus it vanishes if and only if $Q_0 = Q_1$. Second, by the symmetry property of the Hermite average, the symmetry of the connecting curve C is obtained, that is $C_{Q_0,Q_1}(w) = C_{Q_1,Q_0}(1-w)$. Finally, the triangle inequality holds by (4.11). □

Back to the proof of convergence for the $m = 1$ case of Algorithm 4 with $H_{\frac{1}{2}}$ replacing $\mathcal{DH}_{\frac{1}{2}}$. Using the notation there, we have for any $i \in \mathbb{Z}$:

$$\mathcal{L}_H(Q_i^1, Q_{i+1}^1) \le \max_{j=0,1} \mathcal{L}_H(H_{\frac{1}{2}}(Q_i^0, Q_{i+1}^0), Q_j) \le \mu \mathcal{L}_H(Q_i^0, Q_{i+1}^0). \tag{4.13}$$

Since this scheme is interpolatory, contractivity, as obtained in (4.13), is sufficient for convergence. □

We need one further condition for a more general result for higher order m.

Theorem 4.8. *Under the assumptions of Theorem 4.6, if*

$$\mathcal{L}_H(H_{\frac{1}{2}}(Q_0, Q_1), Q_j) = \frac{1}{2}\mathcal{L}_H(Q_0, Q_1), \quad j = 0, 1. \tag{4.14}$$

Then, for any $m \in \mathbb{N}$, the manifold-Hermite Lane-Riesenfeld of order m, $\mathcal{M}_H LR_m$ converges from any admissible initial Hermite data.

Proof. Let $1 < \ell \le m$ and observe step 7 of Algorithm 4 using (4.14) and the triangle inequality,

$$\begin{aligned}\mathcal{L}_H(Q_i^\ell, Q_{i+1}^\ell) &\le \mathcal{L}_H(Q_i^\ell, Q_{i+1}^{\ell-1}) + \mathcal{L}_H(Q_{i+1}^{\ell-1}, Q_{i+1}^\ell)\\ &= \mathcal{L}_H(H_{\frac{1}{2}}(Q_i^{\ell-1}, Q_{i+1}^{\ell-1}), Q_{i+1}^{\ell-1}) + \mathcal{L}_H(Q_{i+1}^{\ell-1}, H_{\frac{1}{2}}(Q_{i+1}^{\ell-1}, Q_{i+2}^{\ell-1}))\\ &= \frac{1}{2}\mathcal{L}_H(Q_i^{\ell-1}, Q_{i+1}^{\ell-1}) + \frac{1}{2}\mathcal{L}_H((Q_{i+1}^{\ell-1}, Q_{i+2}^{\ell-1}))\\ &\le \sup_j \mathcal{L}_H(Q_j^{\ell-1}, Q_{j+1}^{\ell-1}).\end{aligned} \tag{4.15}$$

Therefore, the contractivity factor μ, obtained from the first averaging step (which is the only averaging step in the case $m = 1$) remains valid. In fact, it is now $\mu = 1/2$, and we have,

$$\sup_i \mathcal{L}_H(Q_i^m, Q_{i+1}^m) \le \sup_i \mathcal{L}_H(Q_i^{m-1}, Q_{i+1}^{m-1}) \le \cdots \le \sup_i \mathcal{L}_H(Q_i^1, Q_{i+1}^1) \le \frac{1}{2}\sup_i \mathcal{L}_H(Q_i^0, Q_{i+1}^0).$$

Next, for the D-S condition, we need to show that for any $m \in \mathbb{N}$ there exists a constant C_m such that

$$\mathcal{L}_H(Q_{2j}^m, Q_j^0) \le C_m \Delta\mathbf{Q^0}. \tag{4.16}$$

Here by $\Delta\mathbf{Q^0} = \sup_i \mathcal{L}_H(Q_i^0, Q_{i+1}^0)$. Indeed, since $m > 1$

$$\begin{aligned}\mathcal{L}_H(Q_{2j}^m, Q_j^0) &\le \mathcal{L}_H(Q_{2j}^m, Q_{2j}^{m-1}) + \mathcal{L}_H(Q_{2j}^{m-1}, Q_j^0)\\ &= \frac{1}{2}\mathcal{L}_H(Q_{2j}^{m-1}, Q_{2j+1}^{m-1}) + \mathcal{L}_H(Q_{2j}^{m-1}, Q_j^0)\\ &\le \frac{1}{4}\sup_j \mathcal{L}_H(Q_{2j}^0, Q_{2j+1}^0) + \mathcal{L}_H(Q_{2j}^{m-1}, Q_j^0) \le \frac{1}{4}\Delta\mathbf{Q^0} + \mathcal{L}_H(Q_{2j}^{m-1}, Q_j^0)\end{aligned}$$

Therefore, if we denote $\eta_m = \mathcal{L}_H(Q_{2j}^m, Q_j^0)$ we have

$$\eta_m \le \frac{1}{4}\Delta\mathbf{Q^0} + \eta_{m-1}, \quad \text{where} \quad \eta_1 \le \frac{1}{2}\Delta\mathbf{Q^0}.$$

Therefore, we obtain a finite $C_m = \frac{m+1}{4}$, as required in (4.16). Therefore, we conclude convergence based on the contractivity and D-S. □

One consequence of the assumptions in Theorem 4.8 is that we can apply Theorem 4.2 to our scheme to obtain:

Corollary 4.9. *Under the assumptions in Theorem 4.8, assume that $\mathcal{M}_H LR_m$ is defined using the average H_w. Then, it has an approximation order of (at least) $O(h)$.*

We conclude this part with a few final remarks:

1. The Assumptions on $\mathcal{L}_H$, and in particular (4.11) and (4.14), together with its definition, suggest that $\mathcal{L}_H$ and H_w satisfy the metric property (4.4), basically means that $C(w)$ of (4.9) serves as a geodesic in this abstract metric space, with the metric $\mathcal{L}_H$.
2. With the above in mind, recall Fig. 1 where the first example is of a geodesic in the cone of positive definite matrices. On the contrary, in the second example, we changed the tangents, which gave rise to averaged matrices outside the geodesic. Interestingly, if our average would behave as H_w, we can also view the second example as a geodesic line. Now, however, it is in the abstract metric space of manifold-Hermite data with $\mathcal{L}_H$.
3. If one is interested only in the convergence of $\mathcal{M}_H LR_m$ based on H_w, the condition (4.14) above can be slightly weakened so it will still keep the contractility gained in the first round of averaging. For example, if we only focus on $\mathcal{M}_H LR_2$, we can require that in (4.15)

$$\mathcal{L}_H(H_{\frac{1}{2}}(Q_i^{\ell-1}, Q_{i+1}^{\ell-1}), Q_i^{\ell-1}) + \mathcal{L}_H(H_{\frac{1}{2}}(Q_i^{\ell-1}, Q_{i+1}^{\ell-1}), Q_{i+1}^{\ell-1}) \le \widetilde{\mu}\sup_j \mathcal{L}_H(Q_j^{\ell-1}, Q_{j+1}^{\ell-1}),$$

such that $\mu\widetilde{\mu} < 1$.

CRediT authorship contribution statement

Hofit Ben-Zion Vardi: Formal analysis, Software, Writing – review & editing. **Nira Dyn:** Conceptualization, Validation, Writing – review & editing. **Nir Sharon:** Conceptualization, Formal analysis, Funding acquisition, Investigation, Methodology, Project administration, Resources, Supervision, Validation, Visualization, Writing – original draft, Writing – review & editing.

Declaration of competing interest

The authors of this manuscript declare that they have no conflicts of interest to disclose regarding the research presented in this article. Specifically, no financial interests, relationships, affiliations, or activities could be perceived as having influenced the work reported in this paper.

Data availability

No data was used for the research described in the article.

Acknowledgement

The third author is partially supported by the NSF-BSF award 2019752 and by the DFG award 514588180.

Appendix A. The proof of Lemma 3.9

Proof. We prove the inequality for $d_{\mathcal{M}}\left(p_0,q\right)$, where the other case $d_{\mathcal{M}}\left(p_1,q\right)$ is completely symmetric and follows the same arguments.

By the triangle inequality and the metric property (4.4) we have

$$\begin{aligned} d_{\mathcal{M}}\left(p_0^0,q\right) &\le d_{\mathcal{M}}\left(p_0^0,p_0^1\right)+d_{\mathcal{M}}\left(p_0^1,p_0^2\right)+d_{\mathcal{M}}\left(p_0^2,q\right) \\ &\le \frac{1}{2}d_{\mathcal{M}}\left(p_0^0,p_1^0\right)+\frac{1}{2}d_{\mathcal{M}}\left(p_0^1,p_1^1\right)+\frac{1}{2}d_{\mathcal{M}}\left(p_0^2,p_1^2\right). \end{aligned}$$

Now, we bound separately each of the last two terms above. Before, we note that $d_{\mathcal{M}}\left(p_0^0,p_1^0\right)=\alpha(Q_0,Q_1)$. Next,

$$\begin{aligned} d_{\mathcal{M}}\left(p_0^1,p_1^1\right) &\le d_{\mathcal{M}}\left(p_0^1,p_1^0\right)+d_{\mathcal{M}}\left(p_1^0,p_1^1\right) \\ &\le \frac{1}{2}d_{\mathcal{M}}\left(p_0^0,p_1^0\right)+\frac{1}{2}d_{\mathcal{M}}\left(p_1^0,p_2^0\right) \\ &\le \frac{1}{2}\alpha(Q_0,Q_1)+\frac{1}{2}d_{\mathcal{M}}\left(p_1^0,p_2^0\right). \end{aligned}$$

Finally, noting that $\alpha(Q_0,Q_1)=\alpha(Q_1,Q_0)$, we get

$$\begin{aligned} d_{\mathcal{M}}\left(p_0^2,p_1^2\right) &\le d_{\mathcal{M}}\left(p_0^2,p_1^1\right)+d_{\mathcal{M}}\left(p_1^1,p_1^2\right) \\ &\le \frac{1}{2}d_{\mathcal{M}}\left(p_0^1,p_1^1\right)+\frac{1}{2}d_{\mathcal{M}}\left(p_1^1,p_2^1\right) \\ &\le \frac{1}{2}\alpha(Q_0,Q_1)+\frac{1}{2}d_{\mathcal{M}}\left(p_1^0,p_2^0\right). \end{aligned}$$

Summing the above bounds leads to the bound of the lemma. □

Appendix B. The proof of Theorem 4.3

Let $v_1,v_2\in\mathbb{R}^n$ be nonzero vectors. We denote by $\angle(v_1,v_2)=\arccos(\langle\frac{v_1}{\|v_1\|},\frac{v_2}{\|v_2\|}\rangle)$ the small angle between the two directions. In the following, we assume $\mathcal{M}\subset\mathbb{R}^n$ and view the tangent vectors to the manifold curve as vectors in $\mathbb{R}^n$.

To prove the Theorem, we need a few auxiliary results. The settings of the following lemma are illustrated in Fig. B.5.

Lemma B.1. *Let $p,r\in\mathcal{M}\subset\mathbb{R}^n$ and $q\in\mathbb{R}^n$. Assume that there exist c_1 and c_2 such that*

$$c_1\cdot d\le d_{\mathcal{M}}(p,r),\ \|q-r\|\le c_2\cdot d \quad \text{and} \quad \|q-p\|=O(d^2).$$

Then, for sufficiently small d where q is within the injectivity radius from r, we have

$$\angle(p\ominus r,q-r)=O(d) \quad \text{and} \quad \angle(r\ominus p,r-q)=O(d), \tag{B.1}$$

where $p\ominus r$ and $r\ominus p$ are considered as vectors in $\mathbb{R}^n$.

Proof. A smooth normal curve $c(s)$ can be expressed as $c(s)=\dot{c}(0)(s-0)+O(s^2)$. In this case, we consider c to be the geodesic running from r to p. Furthermore, we consider the triangle connecting r, q, and $\dot{c}(0)s$. Here, $\dot{c}(0)=p\ominus r$ is treated as a vector in $\mathbb{R}^n$. The above triangle has two sides of a length of order d; specifically, one is of length $d_{\mathcal{M}}(r,p)$ and the other $\|r-q\|$. The

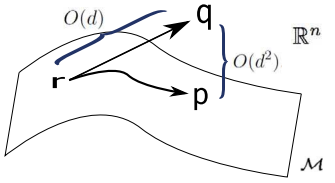

Fig. B.5. An illustration of the settings in Lemma B.1.

opposite side to r in this triangle is of size $\|\dot{c}(0)-q\|$ and is bounded by $\|p-q\|+\|\dot{c}(0)-p\|$, both of length $c\cdot d^2$. Therefore, $\sin\angle(p\ominus r, q-r)=O(d)$ and so for small d we have $\angle(p\ominus r, q-r)=O(d)$.

For the second inequality, we firstly observe that $\angle(p\ominus r, q-r)=\angle(-p\ominus r, r-q)$ and so by the first claim, we have that $\angle(-p\ominus r, r-q)=O(d)$. Next, it holds that $-p\ominus r$ is tangent to the geodesic at r to the opposite direction from p, that is, the vector $PT_{\mathcal{M}}(p; r\ominus p, r)$. Now, when considering the change in tangents over a geodesic, this variation is bounded by the *reach* of $\mathcal{M}$ and the distance along the geodesic, see Boissonnat et al. (2019, Lemma 5). Specific, $\angle(PT_{\mathcal{M}}(p; r\ominus p, r), r\ominus p)=O(d)$. To summarize:

$$\begin{aligned}\angle(r\ominus p, r-q) &\le \angle(r\ominus p, -p\ominus r)+\angle(-p\ominus r, r-q)\\ &\le \angle(r\ominus p, PT_{\mathcal{M}}(p; r\ominus p, r))+\angle(p\ominus r, q-r)=O(d)\end{aligned}$$ □

Next, we provide a lower bound on the distance between our averages and the initial points.

Lemma B.2. *Consider the four control points (2.4) of the Hermite average in $\mathbb{R}^n$ where we denote the endpoints by p_0 and p_1 and their distance by $\|p_0-p_1\|=d$. Assume the corresponding vectors in (2.4) are of lengths $\|v_j\|=\frac{1}{3}d+\varepsilon_j$, $j=0,1$ where $\varepsilon_0+\varepsilon_1<\frac{2}{3}d$. Then, the Bézier average b satisfies*

$$\|b-p_0\|\ge\frac{1}{4}d-\frac{3}{8}(\varepsilon_0+\varepsilon_1)>0. \tag{B.2}$$

Proof. As a first step, without loss of generality, since the entire calculation process is based on linear combinations of the four control points, we can, for simplicity, restrict the proof to $\mathbb{R}^3$. In addition, since this process is invariant to rigid motion, we use $p_0=0$ and $p_1=(d,0,0)$. Then, in a direct calculation, we obtain that the Bézier average for these settings is $b=\frac{1}{2}p_1+\frac{3}{8}(v_0+v_1)$.

As a second step, we denote a given vector u and a value ℓ such that $\ell<\|u\|$ and consider the following convex problem:

$$\begin{aligned}\min_x\quad & \|u+x\|^2\\ \text{s.t.}\quad & \|x\|\le\ell\end{aligned}$$

The solution is obtained on the boundaries of the domain where $x=-\ell\frac{u}{\|u\|}$. In our case, since $\varepsilon_0+\varepsilon_1<\frac{2}{3}d$ we get that

$$\left\|\frac{3}{8}(v_0+v_1)\right\|\le\frac{1}{4}d+\frac{3}{8}(\varepsilon_0+\varepsilon_1)<\frac{1}{2}d.$$

Therefore, if we consider $u=\frac{1}{2}p_1=(\frac{d}{2},0,0)$, we have that $\min\|b\|$ is $\frac{1}{4}d-\frac{3}{8}(\varepsilon_0+\varepsilon_1)$, obtained at the point $(\frac{1}{4}d-\frac{3}{8}(\varepsilon_0+\varepsilon_1),0,0)$. Since $p_0=0$, the result follows. □

Recall that the calculation of the Bézier average is symmetric between the endpoints, and so the above lemma can be concluded in a broader context:

Corollary B.3. *Using the notation of Lemma B.2, we assume $\varepsilon_0+\varepsilon_1$ are bounded away from $\frac{2}{3}d$, that is, there exists A such that $\varepsilon_0+\varepsilon_1<A<\frac{2}{3}d$. Then, there exists a constant $c\in(0,\frac{1}{4})$, independent of the endpoints, such that*

$$\|b-p_j\|\ge c\cdot d,\quad j=0,1.$$

In addition, for d small enough, one can derive a similar bound for the De Casteljau average.

The second part of Corollary B.3 is based on Lemma 3.7, since the two averages there are of distance of order d^2.

We are now ready for the main proof:

Proof of Theorem 4.3. The first claim, that is (4.7), appears as a special case of Lemma 3.7 with $w=\frac{1}{2}$. Next, we show two of the four cases in (4.8), where the other two are completely analogous and are based on the same arguments.

For the first, we use triangle inequality and the first claim of Lemma B.1 to obtain

$$\begin{aligned}\theta_0(Q_0, Q_{\frac{1}{2}}) &= \angle(v_0, q \ominus p_0)\\ &\le \angle(v_0, b - p_0) + \angle(b - p_0, q \ominus p_0)\\ &= \theta_0^E(Q_0, B_{\frac{1}{2}}) + O(d).\end{aligned}$$

For the second angle, we start by estimating the angle between the two new tangents using the following:

$$\angle(u, v) \le \angle(u, q \ominus p_0^2) + \angle(q \ominus p_0^2, p_1^2 - p_0^2) + \angle(p_1^2 - p_0^2, v). \tag{B.3}$$

To evaluate the right-hand side, we note three observations. First, since $\theta_j^E(Q_0, Q_1) \ll 1$, we have $\alpha(\beta_0^0, \beta_0^3) \approx 1/3$. Therefore, by carefully following the De Casteljau algorithm, we obtain that $\left\|\beta_1^2 - \beta_0^2\right\| \approx d/3 = O(d)$ in such cases. Moreover, by Corollary B.3, and by the proximity of the points in the process, we get that $\left\|p_1^2 - p_0^2\right\| \approx C \cdot d$, for some constant C. Recall that the direction of v is the same as $\beta_1^2 - \beta_0^2$ (De Casteljau in Euclidean space), and therefore, we consider a vector of the direction v and of size $\left\|\beta_1^2 - \beta_0^2\right\|$ to p_0^2 to obtain a triangle. Thus, we have a triangle with sides of length of order d, and the angle is $\angle(p_1^2 - p_0^2, v) = O(d)$ since it is located in front of a side of size $O(d^2)$ (we shifted $\beta_1^2 - \beta_0^2$ to a distance of $O(d^2)$ and the distance between β_1^2 and p_1^2 is bounded by $O(d^2)$) and so, as in the proof of Lemma B.1, its sinus is of $O(d)$. The third observation is that $q \ominus p_0^2$ is a parallel transport of u over a geodesic of length bounded by $O(d)$ and thus $\angle(u, q \ominus p_0^2) = O(d)$ and we finalize our bound over the right-hand side of (B.3) by applying the first claim of Lemma B.1 and obtaining $\angle(u, v) \le O(d)$.

For the second bound, and similarly to the first bound, we again use a triangle inequality, and now with the second claim of Lemma B.1:

$$\begin{aligned}\theta_1(Q_0, Q_{\frac{1}{2}}) &= \angle(u, p_0 \ominus q)\\ &\le \angle(u, v) + \angle(v, p_0 - b) + \angle(p_0 - b, p_0 \ominus q)\\ &= O(d) + \theta_1^E(Q_0, B_{\frac{1}{2}}) + O(d). \quad \square\end{aligned}$$

References

Beudaert, Xavier, Pechard, Pierre-Yves, Tournier, Christophe, 2011. 5-axis tool path smoothing based on drive constraints. Int. J. Mach. Tools Manuf. 51 (12), 958–965.

Boissonnat, Jean-Daniel, Lieutier, André, Wintraecken, Mathijs, 2019. The reach, metric distortion, geodesic convexity and the variation of tangent spaces. J. Appl. Comput. Topol. 3, 29–58.

Crouch, Peter, Kun, G., Leite, F. Silva, 1999. The De Casteljau algorithm on Lie groups and spheres. J. Dyn. Control Syst. 5 (3), 397–429.

Dekster, Boris V., 1977. Estimates of the length of a curve. J. Differ. Geom. 12 (1), 101–117.

Dekster, Boris V., 1980. The length of a curve in a space of curvature $\le k$. Proc. Am. Math. Soc. 79 (2), 271–278.

Dokken, Tor, Dæhlen, Morten, Lyche, Tom, Mørken, Knut, 1990. Good approximation of circles by curvature-continuous Bézier curves. Comput. Aided Geom. Des. 7 (1–4), 33–41.

Dyn, Nira, Sharon, Nir, 2017a. A global approach to the refinement of manifold data. Math. Comput. 86 (303), 375–395.

Dyn, Nira, Sharon, Nir, 2017b. Manifold-valued subdivision schemes based on geodesic inductive averaging. J. Comput. Appl. Math. 311, 54–67.

Hofit, Ben-Zion Vardi, Nira, Dyn, Nir, Sharon, 2023. Geometric Hermite interpolation in r n by refinements. Adv. Comput. Math. 49 (3), 38.

Lipovetsky, Evgeny, Dyn, Nira, 2016. A weighted binary average of point-normal pairs with application to subdivision schemes. Comput. Aided Geom. Des. 48, 36–48.

López, M. Castrillón, Fernández Mateos, V., Munoz Masqué, J., 2010. Total curvature of curves in Riemannian manifolds. Differ. Geom. Appl. 28 (2), 140–147.

Moosmüller, Caroline, 2016. C^1 analysis of Hermite subdivision schemes on manifolds. SIAM J. Numer. Anal. 54 (5), 3003–3031.

Moosmüller, Caroline, 2017. Hermite subdivision on manifolds via parallel transport. Adv. Comput. Math. 43 (5), 1059–1074.

Nava-Yazdani, Esfandiar, Polthier, Konrad, 2013. De Casteljau's algorithm on manifolds. Comput. Aided Geom. Des. 30 (7), 722–732.

Park, F.C., Ravani, B., 1995. Be´zier curves on Riemannian manifolds and Lie groups with kinematics applications. J. Mech. Des. 117 (1), 36–40.

Petersen, Peter, 2006. Riemannian Geometry, vol. 171. Springer.

Rodrigues, Rui C., Leite, F. Silva, Jakubiak, Janusz, 2005. A new geometric algorithm to generate smooth interpolating curves on Riemannian manifolds. LMS J. Comput. Math. 8, 251–266.

Vargas, Arturo, Hagstrom, Thomas, Chan, Jesse, Warburton, Tim, 2019. Leapfrog time-stepping for Hermite methods. J. Sci. Comput. 80 (1), 289–314.

Wallner, Johannes, Dyn, Nira, 2005. Convergence and c1 analysis of subdivision schemes on manifolds by proximity. Comput. Aided Geom. Des. 22 (7), 593–622.

Xu, Lianghong, Shi, Jianhong, 2001. Geometric Hermite interpolation for space curves. Comput. Aided Geom. Des. 18 (9), 817–829.

Zhang, Erchuan, Noakes, Lyle, 2019. The cubic de Casteljau construction and Riemannian cubics. Comput. Aided Geom. Des. 75, 101789.

Zimmermann, Ralf, 2020. Hermite interpolation and data processing errors on Riemannian matrix manifolds. SIAM J. Sci. Comput. 42 (5), A2593–A2619.

Zimmermann, Ralf, 2021. Manifold interpolation. In: Benner, P., Grivet-Talocia, S., Quarteroni, A., Rozza, G., Schilders, W., Silveira, L.M. (Eds.), System- and Data-Driven Methods and Algorithms. In: Model Order Reduction, vol. 1, pp. 229–274.

Zimmermann, Ralf, Bergmann, Ronny, 2023. Multivariate Hermite interpolation on Riemannian manifolds. SIAM J. Sci. Comput.